Optical non-linearity in liquid crystals using surface plasmon-polaritons

1989 J. Phys.: Condens. Matter 1 6231

(http://iopscience.iop.org/0953-8984/1/35/021)

J. Phys.: Condens. Matter 1 (1989) 6231–6260. Printed in the UK

Optical non-linearity in liquid crystals using surface plasmon–polaritons

R A Innes and J R Sambles

Thin Film and Interface Group, Department of Physics, University of Exeter, Stocker Road, Exeter EX4 4QL, Devon, UK

Received 13 October 1988

Abstract. We present a detailed report of the observation of a strong, thermally induced optical non-linearity in a system comprised of a silver film and a nematic liquid crystal, in which the surface plasmon–polariton (SPP) mode may be excited. Various measurements of the reflected intensity from the experimental system as a function of the incident angle, including a novel 'AC-on-DC' probe technique, reveal that the observed sharp optical switching is due to warming of liquid crystal, close to the metal/liquid crystal interface, into the isotropic phase through loss of energy of SPPs in Joule heating of the silver film. The many factors contributing to the observed reflectances are investigated and lead to a detailed model of the non-linearity for which a computer model is constructed. Conclusions drawn from the results of this work have serious implications for the use of SPPs in non-linear optics.

1. Introduction

The electronic structure of liquid crystals is mainly dominated by that of individual molecules, and so the electronic contribution to optical non-linearity is essentially the same as that in other organic liquids. Second- and third-harmonic generation (Arakelyan *et al* 1981, Shelton and Shen 1970) have both been observed but it is the intensity-dependent refractive index of liquid crystals that has attracted most attention over the past ten years—self-focusing (Zel'dovich *et al* 1980), degenerate four-wave mixing (Durbin *et al* 1982), phase conjugation (Khoo and Zhuang 1982) and optical bistability (Khoo 1982) have all been observed. Most work has concentrated upon optical bistability in liquid crystals (with its obvious application to optical switching elements, Abraham and Smith 1982) using CW laser beams focused ($\sim$ 10–100 W cm^{-2} intensity) onto the cell, usually contained within a Fabry–Perot cavity to enhance the radiation intensity. Optical bistability may then be observed through the non-linear response of the liquid crystal with change in intensity, due either to reorientation of the director (average molecular orientation) with the optical electric field or laser-induced heating.

In the nematic phase, although the optical field is not strong enough to modify the degree of molecular alignment significantly (as is the case in the isotropic phase (Khoo and Shen 1985), it is sufficient to reorientate the direction of alignment. Due to the correlated molecular response, the resulting change in the refractive indices is large but slow. DC and AC fields being equivalent in reorientating molecules (provided no permanent dipoles exist) means that a laser beam intensity of $\sim$ 250 W cm^{-2} (E =

0953-8984/89/356231+30$02.50

300 V cm^{-1}) is capable of inducing an average refractive index change of 0.01–0.1 in a nematic film (Khoo and Shen 1985) but the response time may be more than a few seconds.

Propagation of a 350 W cm^{-2} CW argon ion laser beam through a 100 μm film of liquid crystal results in a temperature rise of ~2 K on the beam axis (Durbin 1984). The refractive index change due to heating, although similar to other organic liquids in the isotropic phase (and in the nematic phase well below the clearing point) increases significantly as the clearing point is approached from below, perhaps resulting in a change of 0.03 in the extraordinary refractive index for a 2 K rise in temperature, just below the clearing point. A much larger Δn may be achieved if the liquid crystal is warmed through the clearing point ($\Delta n \sim 0.05$). The response time for this laser-induced heating is significantly shorter than that of molecular reorientation and is 10–100 ms (Khoo and Shen 1985).

Both molecular reorientation with the optical field and laser-induced heating may occur simultaneously, although their relative strengths will depend upon the experimental configuration used. Provided no significant absorber is present, molecular reorientation will generally dominate. However, if a metal, for example, is introduced, heating will become significant and may dominate (Sambles and Innes 1988, Lloyd *et al* 1987). One such configuration, in which heating is very significant, involves the use of the surface plasmon-polariton mode (Innes and Sambles 1987).

2. Surface plasmon–polaritons

A surface plasmon–polariton (SPP) is a coupled electromagnetic-field CDW that may occur at the interface between a dielectric ($\epsilon_d > 0$) and a medium whose optical dielectric constant ($\epsilon = \epsilon_r + i\epsilon_i$) has $\epsilon_r < 0$. At any frequency, the momentum of an electromagnetic wave incident in a dielectric is always less than that of the localised SPP mode at that dielectric/metal interface. Thus it is impossible to couple the incident radiation directly into the SPP from the dielectric. The 'missing' momentum may be supplied by using the technique of attenuated total reflection (ATR) coupling in either the Otto (1968) or Kretschmann–Raether (Kretschmann and Raether 1968) configurations, both of which involve the metal/dielectric interface being placed at a suitable distance from a prism within which a light beam is being totally internally reflected.

The wavevector along the interface of the evanescent wave present at total reflection is

$$k_x = nk \sin \theta \tag{1}$$

where n is the refractive index of the prism, $k = 2\pi/\lambda$ and θ is the angle of incidence of the light at the interface. By altering θ or k it is possible for both energy and momentum to be conserved and the p-polarised light (SPPs are TM modes (Boardman 1982)) may couple into the SPP mode. Usually, measurements are made of the reflected intensity from the sample as a function of angle of incidence. At a particular incident angle, θ_{SPP}, a dip in the reflected intensity occurs due to the excitation of the SPP mode and subsequent loss of energy through Joule heating of the metal (Innes and Sambles 1985).

Coupling of incident radiation to the SPP mode is a resonant phenomenon. Satisfaction of the resonance condition results in high field intensities (Innes *et al* 1987)

localised at the interface, not only making the SPP a sensitive surface tool, but it also has potential in non-linear optics allowing, in theory, the observation of optical bistability in reflection. However, unlike the resonances of a Fabry–Perot cavity, the SPP resonance is not simply a change in reflectance and transmittance of the system but rather nearly all the power is converted into Joule heating of the metal film. Therefore, with relatively low incident photon powers, focused to perhaps an area of $\sim 5 \times 10^4$ μm^2, there will be substantial heating of the film, the volume of metal thermally excited being $\sim 4 \times 10^{-15}$ m^3 in the Kretschmann–Raether configuration. With strong local heating and an adjacent material with a substantial temperature-dependent refractive index, non-linear effects due to heating are inevitable and are likely to dominate. Previous work on the subject has, however, concentrated upon the field enhancement property of SPPs and not on this important thermal aspect.

3. Optical bistability in reflection

Optical bistability in reflection at grazing angle of incidence from the boundary between two media, one of which is optically non-linear, was first theoretically proposed by Kaplan (1977). Experimentally, Smith *et al* (1979) were the first to observe this effect from the boundary between a glass prism and CS_2 — an optical Kerr medium. By operating at angles of incidence close to the critical angle, it was possible to alter the reflectivity of the system by $\sim 20\%$ from totally internally reflecting to transmitting, using the intensity-dependent refractive index of CS_2.

A low-intensity beam, incident through the linear medium at an angle of incidence greater than the critical angle, will undergo total internal reflection at the interface. Although there is no transmitted beam, an evanescent field is present in the non-linear medium. Due to the positive Kerr constant of the medium the evanescent field will increase the refractive index of this medium, thus reducing the critical angle and affecting the phase shift between incident and reflected beams. Such a reduction in the critical angle towards the incident angle results in an increase in amplitude of the evanescent field, producing a positive feedback in which an increase in the incident intensity increases the evanescent field, reducing the effective critical angle and thus further increasing the evanescent field. There will then be a switch, at some critical intensity, from total internal reflection to transmission. Smith *et al* argued that the transmitted beam will act to further increase the index of the non-linear medium so that once the switch to transmission has occurred, an appreciable reduction in the incident intensity will be required to return the system to total reflection. Optical bistability will therefore occur.

Optical bistability was indeed observed with a switching time of ~ 300 ps; times of ~ 2 ps should be possible with CS_2, the limiting factor in these experiments being the response time of the detection system. However, the critical intensity for the observation of optical bistability was $\sim 8 \times 10^9$ W cm^{-2}. In order to reduce the required incident intensity some workers looked at the possibility of using SPPs to enhance the evanescent field.

4. Optical bistability in reflection using SPPs

To understand the principle of optical bistability using SPPs consider the system shown in figure 1, involving a silver film in the Kretschmann–Raether configuration together

with a dielectric (medium 3). With incident radiation of wavelength $\lambda = 632.8$ nm, the dielectric constants of the media are $\epsilon_{prism} = 3.24$, $\epsilon_{Ag}=-17.0+0.7i$ and $\epsilon_3=2.25$ — the silver film is 50 nm thick.

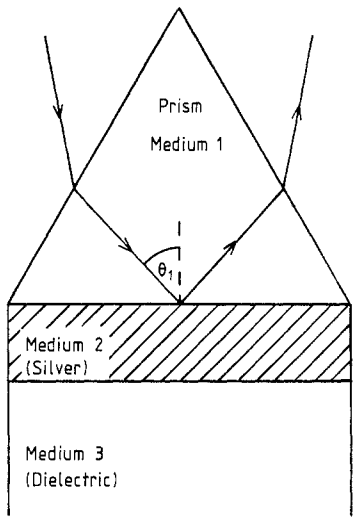

Figure 1. Kretschmann–Raether configuration for exciting an SPP at a metal/non-linear medium (medium 3) interface.

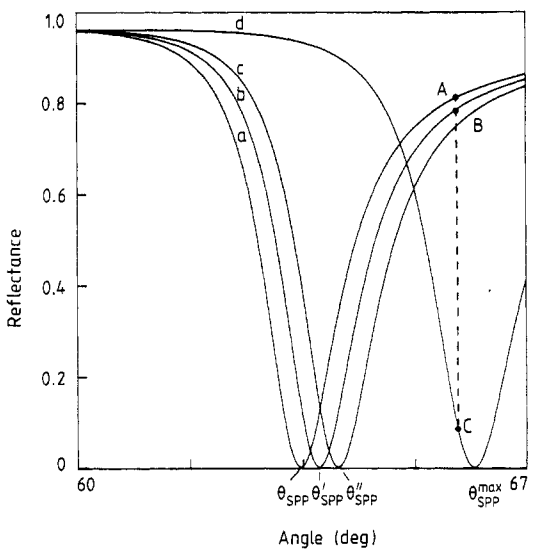

Figure 2. Calculated reflectance curves as a function of incident angle for the system shown in figure 1 for various values of ϵ_3, illustrating the principle of optical bistability. Curve a, $\epsilon_3=2.25$; curve b, $\epsilon_3=2.27$; curve c, $\epsilon_3=2.29$; curve d, $\epsilon_3=2.34$.

Figure 2, curve a, is the expected reflectance against angle of incidence response calculated from Fresnel theory for such a system. If ϵ_3 is now increased in steps from

2.25 to 2.34 then, as figure 2, curves b, c, and d illustrate, the SPP resonance dip moves to higher angles of incidence. Now consider the situation where $\epsilon_3 = \epsilon_3^0 + \alpha|E_3^+|^2$, meaning that the dielectric constant of medium 3 is dependent upon the intensity of the optical electric field in medium 3 (α is a non-linear coefficient, assumed to be positive, and ϵ_3^0 is the dielectric constant for zero incident intensity). Setting $\epsilon_3^0 = 2.25$, the expected reflectance response for zero incident intensity would be that of figure 2, curve a. If the angle of incidence is now kept constant at a value corresponding to point A on curve a and the incident intensity steadily increased, then the amplitude of the evanescent field in medium 3, $|E_3^+|$, will correspondingly start to increase, causing an increase in the dielectric constant of medium 3. Such an increase in ϵ_3 will move the angle of the SPP resonance dip, θ_{SPP}, to a slightly higher angle of incidence, θ'_{SPP}, so that the reflectance of the system will now correspond to point B on curve b. The corresponding increased enhancement will further increase $|E_3^+|$ and θ'_{SPP} will move towards θ''_{SPP}, resulting in still further enhancement. The rate of change of enhancement with increase in intensity increases dramatically as this positive feedback process quickly evolves so that θ_{SPP} will rapidly be drawn to an angle θ_{SPP}^{max}, which is the maximum resonance angle that the fields can maintain for a particular input intensity. The expected reflectance response as a function of incident intensity will therefore be as shown in figure 3, curve a, with a sharp downwards switch at a particular critical intensity, as the resonance dip is drawn to θ_{SPP}^{max}—the reflectance at the bottom of the switch corresponds to that of point C in figure 2. Provided ϵ_3 can be increased further by an increase in the incident intensity, then the reflectance will continue to increase, i.e. θ_{SPP}^{max} continues to increase. If the intensity is now steadily decreased the SPP resonance dip will start to move to lower incident angles, as the amplitude of the electric field in medium 3, $|E_3^+|$, can no longer maintain the high-angle dip. However, in this direction there is a tendency for $|E_3^+|$ to oppose the movement of the resonance dip to lower incident angles. Therefore, the enhancement in $|E_3^+|$ will maintain operation at as high a resonance minimum angle as possible until the incident intensity is decreased sufficiently so that, even with maximum enhancement in $|E_3^+|$, the fields are no longer able to maintain the dip at higher angles of incidence and the sharp upwards switch of figure 3, curve b then occurs, as the system returns to the original low-intensity SPP resonance dip at θ_{SPP}. Optical bistability in reflection using the SPP resonance has thus been achieved.

An alternative to monitoring the reflectance at a fixed angle of incidence with varying incident intensity is that of measuring the reflectance, R, for a series of fixed intensities but variable angle of incidence. The expected form of the data may once again be deduced intuitively using figure 4.

The broken curve of figure 4 is the zero-intensity reflectance response of the system. For angles of incidence lower than θ_{SPP}, it can be seen that for non-zero incident intensities movement of the resonance minimum to a higher angle will occur, causing the reflectance R_i at an incident angle θ_i, to be increased. Therefore when the intensity is switched on, the reflectance minimum will move to the right causing R_i to increase, reducing the enhancement in $|E_3|^+$ and thus causing the minimum to move to the left (but not as far as the initial, zero intensity limit). The amplitude of $|E_3|^+$ will now increase and therefore the minimum will move to the right once again, but not as far as the initial non-zero intensity limit. It can be seen that the system will reach an equilibrium reflection state corresponding to R_i' on the full curve of figure 4. If the angle is swept from low to high angles of incidence, there will be a tendency for the reflectance minimum to be pushed away from the incident angle, and the resonance minimum will move as far to the right of figure 4 as possible until, even with maximum

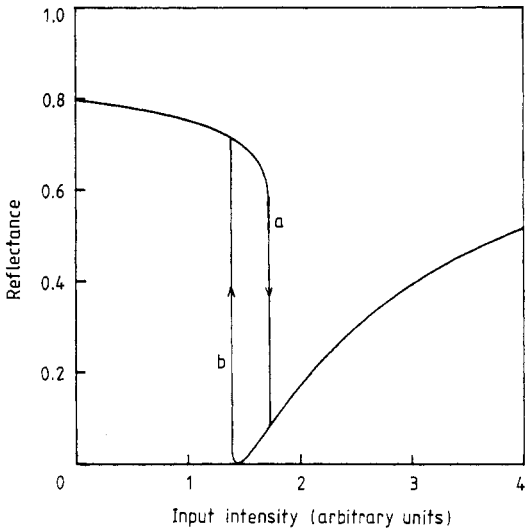

Figure 3. Reflectance as a function of incident intensity for an angle of incidence corresponding to point A in figure 2. Increasing the intensity produces curve a, decreasing gives curve b.

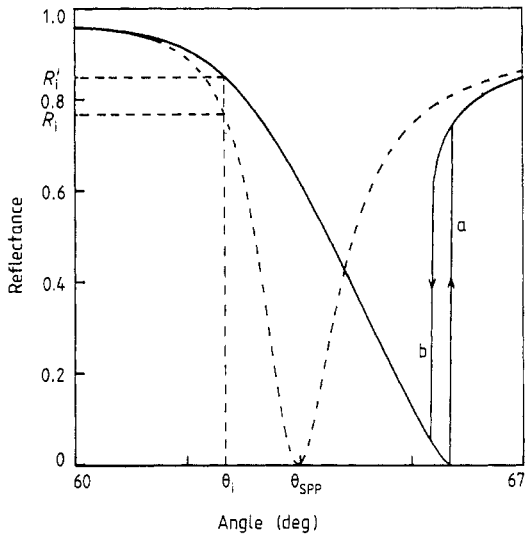

Figure 4. Illustration of the principle behind the observation of optical bistability with incident angle. Increasing the angle produces curve a, decreasing gives curve b.

enhancement in $|E_3|^+$, the field can no longer maintain this resonance minimum and a sharp, upwards switch occurs to a lower intensity minimum.

If the angle of incidence is now decreased then the reflectance will follow the path of the low-intensity response. However, in this direction a positive feedback mechanism does exist so that the increased enhancement in $|E_3|^+$ will quickly draw the minimum to the highest angle of incidence possible and a sharp, downwards switch will occur. Hysteretic behaviour with angle sweep direction is therefore observed; one would

expect the width of the loop to increase with increase in incident intensity.

Wysin *et al* (1981) were the first to consider, theoretically, optical bistability using SPPs in a system, such as shown in figure 1, involving a Kerr effect non-linear medium. Using reflection and transmission coefficients and Snell's law, together with the intensity-dependent dielectric constant, Wysin *et al* were able to obtain expressions for the incident and reflected intensities, $U_{i,r}$, in terms of the intensity in medium 3, U_3. The expressions obtained were too complicated to allow analytical demonstration of the bi-stable nature of the solution but, by firstly assuming values for U_3 for a given θ_1, close to the SPP resonance angle, θ_{SPP}, and then using the expressions to plot U_i and U_r against U_3, the optically bi-stable behaviour of the type shown in figure 3 was obtained. The condition for bistability to occur is that a given value of U_i should correspond with multiple values of U_3 although each value of U_3 should produce a unique value of U_r— hence multiple values of the reflectance are obtained for a single value of U_i. Wysin *et al* furthered their calculation to investigate the behaviour of the critical switching intensity, U_c—the incident intensity required to observe bistability—with initial detuning from θ_{SPP}, i.e. the angular position of point A in figure 2. Their results indicate that the switching intensity increases rapidly with increase in angular offset, since more power is required to move θ_{SPP} to θ_1. They also illustrated the behaviour for negative non-linear media and found it to be similar but, naturally, with opposite angular offset.

A less opaque theoretical consideration of optical bistability with SPPs has been undertaken by Martinot in systems containing CS_2 which, in addition to being a Kerr medium (Martinot *et al* 1984) has a large thermo-optic coefficient, i.e. change in refractive index with temperature (Martinot *et al* 1985). A similar approach will now be described which can easily be programmed into a computer and which may be used to model the experimental results presented later.

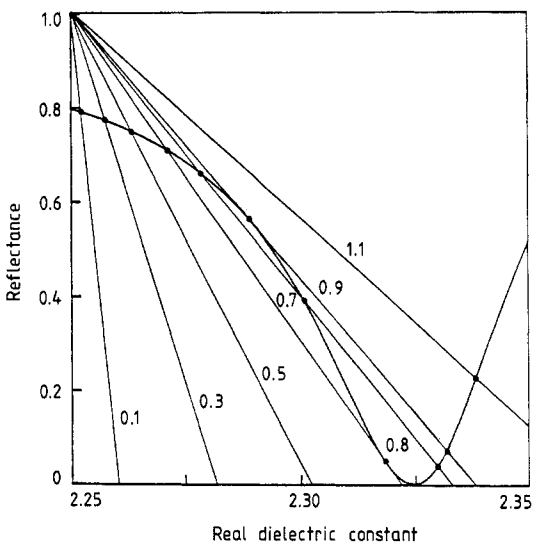

Figure 5. Graphical solution for optical bistability. The numbers correspond to the reciprocal of the gradients of the straight lines (×10).

The variation of R with increase in ϵ_3 from ϵ_3^0, $R_\theta(\epsilon_3)$, at an angle of incidence corresponding to point A in figure 2, is given in figure 5. The intensity-dependent

dielectric constant may be written in a general form

$$\epsilon_3 = \epsilon_3^0 + \alpha I(1 - R - T) \tag{2}$$

I being the incident intensity and α the non-linear coefficient, which will be assumed to be equal to unity. α is essentially the proportionality constant between the change in dielectric constant $\epsilon_3 - \epsilon_3^0$ and the rate of heating per unit area $I(1 - R - T)$, where T is the intensity transmittance. Equation (2) may be written in the form

$$R = (1 - T) - (\epsilon_3 - \epsilon_3^0)/I \tag{3}$$

thus illustrating the linear relationship between R and the increase in dielectric constant (since $\alpha > 0$) with gradient inversely proportional to the incident intensity. Since $R_\theta(\epsilon_3)$ gives the allowed reflectance value for a particular ϵ_3, and equation (3) relates the variation of R with change in ϵ_3 at a particular incident intensity, a graphical solution of $R_\theta(\epsilon_3)$ with equation (2) will yield the reflectance for a particular intensity. Figure 5 shows a family of straight lines corresponding to different incident intensities. Initially, for low incident intensities, there is only one solution for the reflectance until $I = 0.07$ is reached, where two solutions are found. Increasing I further, three solutions are now apparent until $I = 0.09$ when there are, once again, two solutions. Additional increase in intensity then yields only one solution. Thus, for a certain range of intensities, the relationship between R and I is multi-valued, a point which is clarified by plotting the solutions of R as a function of I, as shown in figure 6 (similar to figure 3). Tracing a path along the full curve of figure 6, R is single-valued until point A is reached, where two solutions exist. If the intensity is increased further then R will remain high until point B is reached, where a further increase in I results in there being only one solution for R at a much lower value—note also the increased rate of change of R with I. The reflectance is therefore forced to switch to the lower value and will remain in this state on subsequent increase of the intensity. If the intensity is now decreased, the reflectance will follow the full curve until point C is reached. For intensities below this point the solution for R is a high value. The reflectance, therefore, must switch to this high value (point A) and then retrace its path back along the full curve to $I = 0$. Optical bistability has thus been achieved and it can be seen that although there is a region in which there may be three solutions, only the highest and lowest solutions may be reached. For bistability to occur, it is necessary that the $R_\theta(\epsilon_3)$ curve possesses, in some region, a gradient equal to $1/I$.

Confirmation of the intuitive approach for R versus incident angle data is not as straightforward as for the R versus I data, since although the incident intensity is now constant, a change in angle of incidence alters both R and ϵ_3. It is therefore necessary to use an iterative approach on a computer to obtain the expected reflectance response. The most obvious method of iteration is to calculate R and T at a particular angle of incidence, and then to calculate ϵ_3 using equation (2). If, upon comparing the new ϵ_3 with the previous value, the difference is less than some limit, 10^{-5}, for example, then it is assumed that the solution for this angle has been found. Unfortunately, such an approach will fail in the region of bistability since the routine will find two self-satisfying values, neither of which is a solution, and it will oscillate between them (Innes 1987). Hence, a more sophisticated approach is required. The logic behind such an approach is illustrated in figure 7 and may be explained as follows.

The initial zero-intensity response at angle of incidence θ_i corresponds to a dielectric constant ϵ_3^0 and a reflectance R_i. If ϵ_3^0 is now increased by an arbitrary amount to a

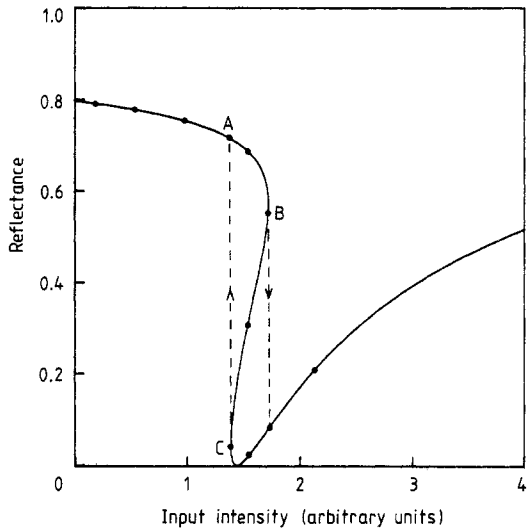

Figure 6. Reflectance versus I response deduced from the graphical solution of figure 5. The dots correspond to the solutions shown in figure 5.

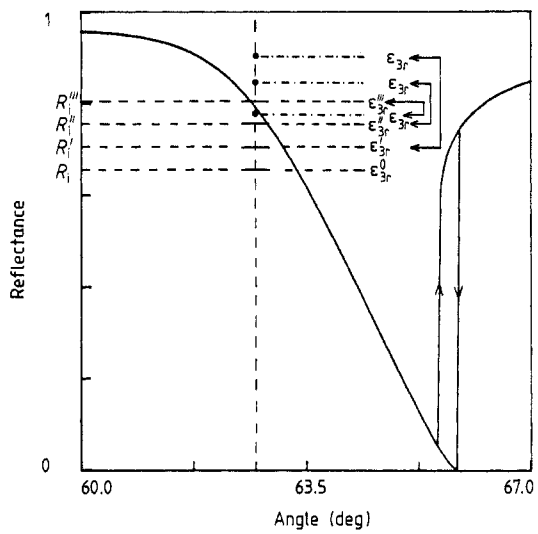

Figure 7. Principle of the iterative computer routine for calculation of the non-linear reflectance response.

value ϵ_3' the reflectance will now be R_1'. Using equation (2) (with $\alpha = 1$ for example) a non-linear dielectric constant ϵ_3 may be calculated using R_1', and comparing ϵ_3 with ϵ_3' it is found that $\epsilon_3 > \epsilon_3'$. Therefore, ϵ_3' is now increased by another increment to ϵ_3'' to give a reflectance R_1''. Using R_1'', ϵ_3 may once again be calculated using equation (2) but, since $R_1'' > R_1'$, the new value of ϵ_3 will lie below the previous value. Comparison of ϵ_3 and ϵ_3'' still gives $\epsilon_3 > \epsilon_3''$. However, ϵ_3'' is now increased to ϵ_3''' and the reflectance, R_1''', $(R_1''' > R_1'' > R_1')$ calculated and substituted into equation (2) to yield ϵ_3 with $\epsilon_3 < \epsilon_3'''$, meaning that the increase in R and the reduction in the absorptance is now

too large to be maintained by the non-linear dielectric, and that the stable solution to the problem has been passed. It is therefore necessary to return to ϵ_3'' and to continue to 'hunt' with a smaller increment in the dielectric constant. A condition similar to $\epsilon_3 < \epsilon_3'''$ will eventually be obtained so that the increments will have to be reduced further until the required precision is achieved. Where there are two stable solutions it is obvious that this routine will hunt only one of them. However, both solutions may be found by firstly searching 'from below' as explained, i.e. commencing from a low value of ϵ_3 and increasing in steps, and then searching 'from above' — commencing from a high value of ϵ_3 and decreasing in steps—for all angles of incidence. Figure 8 shows results from such calculations, illustrating the bi-stable nature of the response for certain intensities and the increase in size of the loop with increase in intensity.

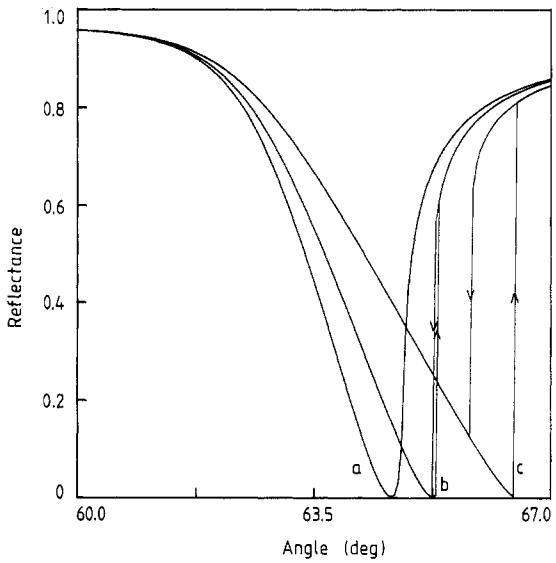

Figure 8. Theoretical non-linear reflectance for three incident intensities. Curve a: I=0.04, no bistability observed; curve b, $I = 0.06$, small bi-stable loop; curve c: $I = 0.10$, illustrating increase in width of loop with increase in intensity.

At this point it is interesting to investigate the influence of the width of the SPP resonance upon the bi-stable behaviour. Intuitively, it should be seen that there is a relationship between the width of the resonance and the change in dielectric constant required to observe bistability. One would expect that the wider the resonance the greater the intensity required for bi-stable operation since, for a given intensity, the fractional shift in the resonance minimum decreases with increase in width. Moreover, with reference to the graphical solution previously presented, greater gradients of R versus ϵ_3 are available with decreasing width of the resonance, implying a higher gain of the positive feedback mechanism, and so one would expect a lower intensity to be required. The truth of this statement is illustrated in figure 9 where, in curve a, the imaginary part of the dielectric constant of the silver has been increased to 1.0, therefore reducing the non-linearity, while in curve b ϵ_{iAg} has been reduced to 0.4, giving rise to a bi-stable loop. This therefore suggests that, for incident radiation in the visible part of the spectrum, silver is the best choice of metal, since its resonance dip is the narrowest.

Finally, it should be noted that all the theoretical analyses of optical bistability using SPPs have assumed the non-linear medium to be homogeneous. However, if SPPs are excited a rigorous treatment must consider an inhomogeneous layered medium problem. Agarwal and Gupta (1986a, b) have furthered the analysis of Wysin *et al* (1981) to account for such a medium, resulting in a doubling of the critical intensities required to observe optical bistability.

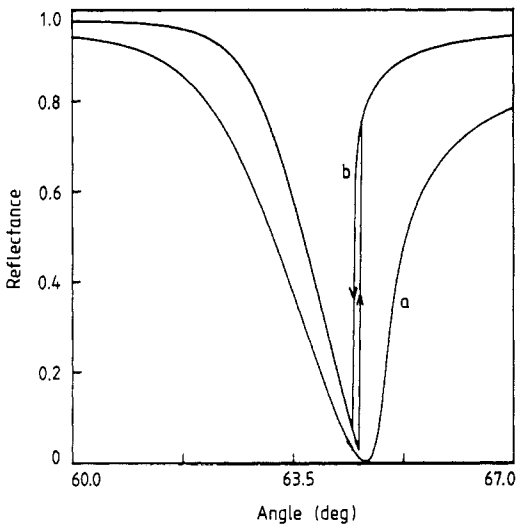

Figure 9. Theoretical non-linear reflectance for an incident intensity of 0.04 for two values of ϵ_{Agi}: (curve a) 1.0, the response is less skew than that of figure 8, curve a; (curve b) 0.4, indicating that the narrower the resonance response the less the critical intensity.

5. Experimental observation of optical bistability using SPPs

Although most of the theoretical work in this field has concentrated upon Kerr media (CS_2 in particular) the two reports on the experimental observation of optical bistability with SPPs, prior to this work, have both been due to thermally induced intensity-dependent refractive indices.

Martinot *et al* (1985) reported the observation of optical bistability in a system comprising a silver film (54.0 nm) sputtered onto a SiO_2 substrate, coated with a layer of SiO_x to protect the silver from chemical attack by the CS_2. Light of wavelength $\simeq$ 600 nm was incident through a hemispherical glass cell containing CS_2 fluid and coupled to the SPP mode along the silver/substrate interface. A 120 mm focal length lens focused the incident radiation onto the silver with a beam waist of $\simeq$ 32 μm. Measurements of the output power as a function of input power were recorded, the results of which, when replotted in terms of reflectance versus power, appear to agree well, qualitatively, with theoretical predictions, bi-stable loops occurring at sufficiently high incident powers. The reflectance was also recorded as the angle of incidence was varied, which showed that although a small bi-stable loop does occur at a power of 21 mW (an intensity at the interface of $\simeq 3 \times 10^3$ W cm^{-2}) the most noticeable effects are the considerable raising and broadening of the reflectance minimum, together with

movement to higher angles of incidence. The authors attributed the movement of the reflectivity minimum to higher angles of incidence to a decrease in the refractive index of the CS_2 'prism' due to heating of the non-linear medium, while the raising and broadening was attributed to the enhanced divergence of the incident and reflected beams induced by temperature gradients near the interface, so that many angles of incidence were present simultaneously. The authors also investigated the switching times of the upwards and downwards switches of the bi-stable loop by varying the input power extremely slowly until switching occurred and recording the intensity on a digital storage oscilloscope. An upwards switching time of $\sim$ 150 ms was measured, while the response time for the downwards switch was determined to be $\sim$ 100 ms. The difference between these two values was thought to be due to the fact that, for the shorter time response, SPPs are better excited and act as a source of heat, while for the upwards jump the heat source disappears as SPPs are no longer excited resonantly and the energy has to propagate away through the system.

The only other experimental report of optical hysteresis using SPPs is that of Arakelyan *et al* (1986) using a system comprising a silver film evaporated onto a high-index glass prism, and a nematic liquid crystal. They observed slight hysteretic behaviour with change in angle of incidence, but only in the SPP reflectance minimum, since the maximum intensity at the interface was estimated to be only $\simeq 6$ W cm^{-2}. The origin of the non-linearity was not discussed.

Having reviewed the limited amount of theoretical and experimental work on the observation of optical bistability using SPPs, it should be obvious that nematic liquid crystals offer the possibility of observations similar to those of Martinot *et al* (1985), either through molecular reorientation or warming of the liquid crystal. The remainder of this paper will investigate a large thermally induced optical non-linearity in a nematic liquid crystal due to the excitation of SPPs (Innes and Sambles 1987) and indeed, results similar to those of Martinot *et al* are obtained although there is a significant difference in interpretation. More sophisticated measurements are also undertaken to improve understanding of all contributory factors.

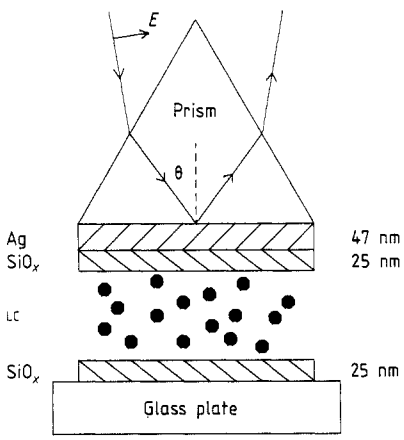

Figure 10. Cross-sectional view of sample geometry showing the nematic liquid crystal director alignment perpendicular to the plane of the paper. With this orientation the liquid crystal presents only one index to the TM radiation.

6. Experimental

Figure 10 is a cross-sectional view of the Kretschmann–Raether sample geometry designed for the observation of optical non-linearities in a nematic liquid crystal. Onto the thin silver film (about 50 nm thick) was evaporated a thin layer of SiO_x (about 25 nm in thickness) which served to align the liquid crystal director in the required direction. An optically flat glass plate, onto which had been evaporated a similar layer of SiO_x, was used to contain and align the liquid crystal so that a homogeneous layer of nematic liquid crystal, with its director aligned perpendicular to the plane of incidence, was obtained. (Further details of sample fabrication are given by Welford *et al* 1987.) Light incident through the high-index glass prism could then couple into the SPP mode along the Ag/SiO_x interface, the fields of which sampled the nematic liquid crystal with dielectric constant $\epsilon_\perp$. Measurements of the reflected intensity from the sample as a function of angle of incidence were then made using standard apparatus (Barnes and Sambles 1986).

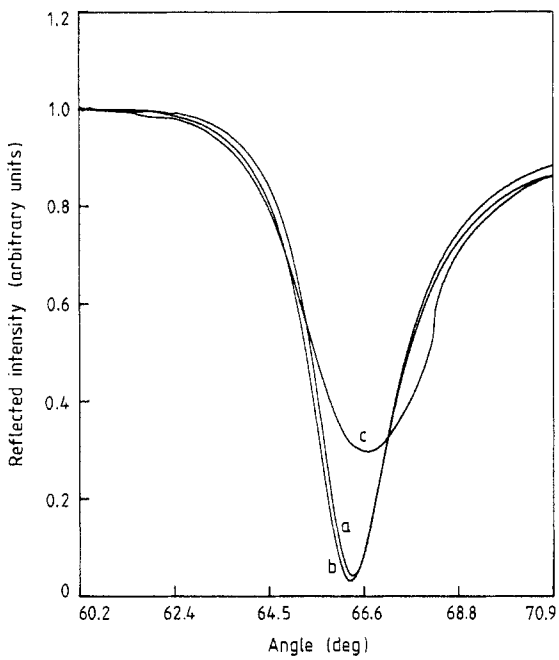

Figure 11. Reflected intensity for: (curve a) 20.5 mW, (curve b) 20 μW focused, (curve c) 20.5 mW focused.

7. Preliminary measurements of optical bistability

7.1. Initial observation

With 20.5 mW He–Ne laser power in a beam of cross-sectional area 0.03 cm^2, incident upon the prism/silver interface, the reflected intensity is that of the linear system as illustrated in figure 11, curve a. For a beam of 20 μW, but focused onto the interface

to a spot size of $\sim 250\ \mu m$, the reflectance response is now that of curve b which, as expected, has a greater half-width than curve a, due to the many angles of incidence now present. The difference, however, is small since the divergence of the beam is not significant in comparison with the width of the resonance dip. If the incident power is now returned to its initial value of 20.5 mW (an intensity at the interface of $\sim 40\ W\ cm^{-2}$) then there is a significant change in the response of the system as illustrated by curve c of figure 11—the SPP resonance dip has risen and broadened considerably and there is an obvious switch at an incident angle of 67.8°. The similarity between this response and that of Martinot *et al* (1985) is striking. The raising and broadening of the resonance dip can be attributed to a Gaussian distribution in the strength of the non-linearity, and also a spread in incident angles caused by focusing. The total response of the system will therefore be an average of the responses of regions of differing intensity-dependent dielectric constant for a range of incident angles.

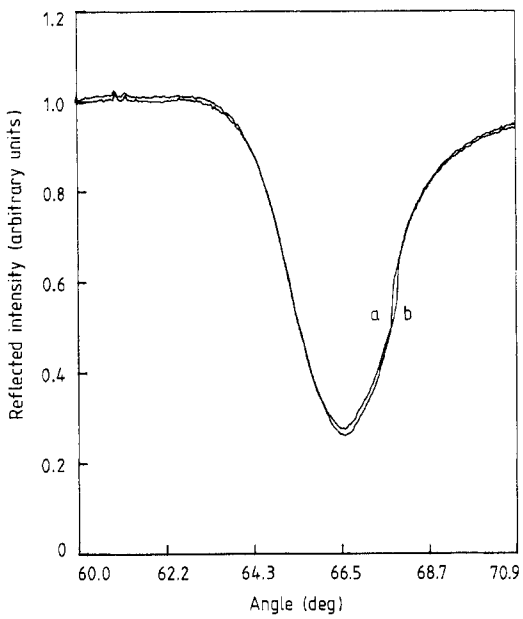

Figure 12. Hysteretic behaviour of reflected intensity with direction of angle sweep: (curve a) high to low angles, (curve b) low to high angles. The lines indicate the angles for the data of figure 13.

All previous data were recorded by sweeping the angle of incidence from high to low angles. If the data are now recorded in the reverse direction with a focused incident beam of 20.5 mW power and then superimposed on the original data, a small hysterisis loop is observed at an angle of $\sim 68°$; figure 12 illustrates this. One would therefore expect measurements of output power against input power to yield optically bi-stable loops at particular angles of incidence. Results of such measurements are presented in figure 13 for a variety of incident angles; as expected, optical hysterisis and bistability are observed.

7.2. Response time of non-linearity

To determine the time of response of this non-linearity a mechanical chopper was introduced to the experimental apparatus so that the incident beam was modulated by

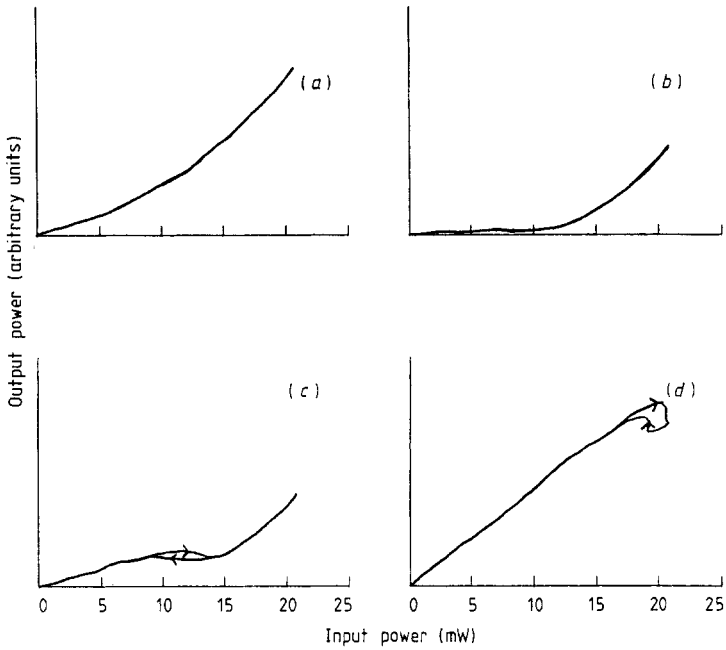

Figure 13. Output power as a function of input power at four incident angles: (*a*) 67.7°, (*b*) 66.6°, (*c*) 67.2°, (*d*) 67.8°. See figure 12 for the positions of these angles with respect to the SPP resonance.

a square wave of 100% depth. The reflected intensity was then recorded at different frequencies of chopping. However, as the frequency was progressively increased, the non-linearity weakened and, at a chopping frequency of 1.25 kHz (see figure 3 of Innes and Sambles (1987)) it has largely disappeared, implying a response time of $\sim$ 20 ms, confirming that the non-linearity is thermally induced.

7.3. Mechanism of non-linearity

It is now important to consider the temperature dependence of $\epsilon_\perp$ for E7 liquid crystal. Figure 14 is a plot of $\epsilon_\perp$ (at $\lambda = 632.8$ nm) against temperature, T, from data supplied by BDH Ltd, the full curves representing the approximations made in the computer modelling. For the temperature range 20–45 °C, $\epsilon_\perp$ remains nearly constant at a value close to 2.304. This immediately implies that the liquid crystal in the experiment must be being warmed by more than 25 °C towards the nematic–isotropic phase transition temperature, $T_c = 58$°C, all measurements presented so far being recorded at room temperature, 20°C. It is therefore interesting to ask whether the increase in the rate of change of $\epsilon_\perp$ between 45°C and 55°C, which may be approximated to a straight line of gradient

$$\alpha = \Delta\epsilon_\perp/\Delta T = 3.3 \times 10^{-3}\,\mathrm{K}^{-1}$$

is sufficient for optical bistability to occur, or whether the liquid crystal must be warmed closer to, or beyond, the clearing-point temperature T_c. The computer model previously described may be utilised to answer this question.

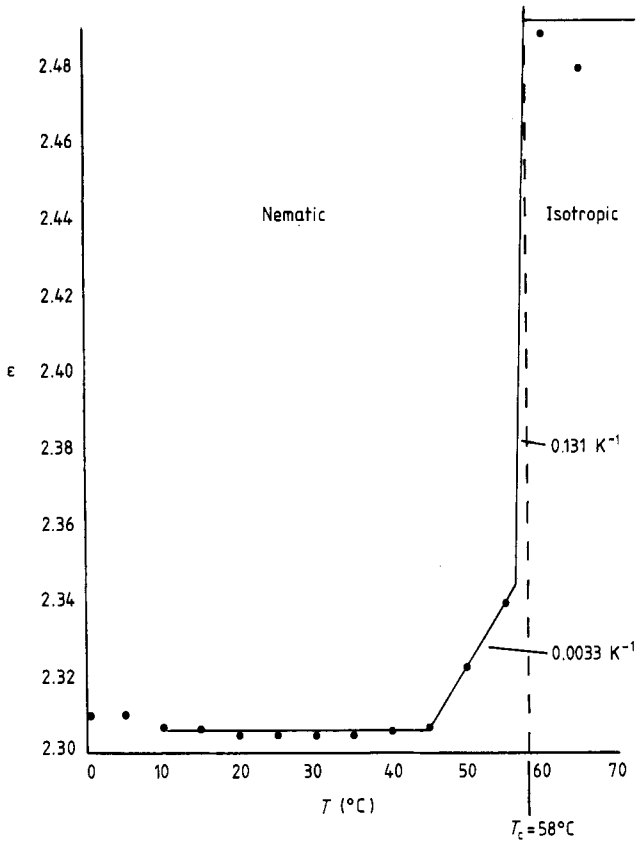

Figure 14. $\epsilon_\perp$ as a function of temperature for E7. The full curves show the approximations made in computer modelling of the non-linearity.

The optical parameters for the experimental system deduced from fitting Fresnel's equations for multilayered systems to the data (Barnes and Sambles 1986) may now be used in computer modelling the non-linear response of the system. Using the value of α stated above and ensuring that the input intensity is not sufficient to raise $\epsilon_\perp$ above a value of 2.3391 (at 55°C) and using an initial value for $\epsilon_\perp = 2.3063$ (at 45°C), it is a simple matter to show that the change in $\epsilon_\perp$ is not sufficient for bistability to occur, although the response is slightly skew. One must then ask what increase in $\epsilon_\perp$ is necessary for optical bistability to occur. Once again, the problem may be resolved using the computer model by simply increasing the value of I until critical switching is observed. Knowing the maximum absorption of the system from the depth of the reflectance minimum it is then possible to calculate the increase in ϵ_3 for a particular α using equation (2). Following this procedure it is found that $\epsilon_\perp = 2.3063$ (at 45°C) must be increased to a value of $\epsilon_\perp = 2.385$ in order to observe optical bistability. According to the straight-line approximations made for the behaviour of $\epsilon_\perp$ with T, illustrated in figure 14, this suggests that the liquid crystal is being warmed to within 1 K of the clearing point. However, the straight-line approximations were made for ease of computing, since it is the net change in $\epsilon_\perp$ that is of most importance, and not the specific profile of that change. It is likely that there exists a large discontinuity in

$\epsilon_\perp$ at T_c (see figure 17). One can therefore conclude that the experimentally observed optical non-linearity is due to warming of the nematic liquid crystal into the isotropic phase. It is immediately apparent that a large proportion of the incident energy in the focused beam is being used to warm the liquid crystal from room temperature without contributing to the non-linearity. Raising the ambient temperature should therefore reduce the intensity required to observe the optical non-linearity and so remove the need for a converging lens.

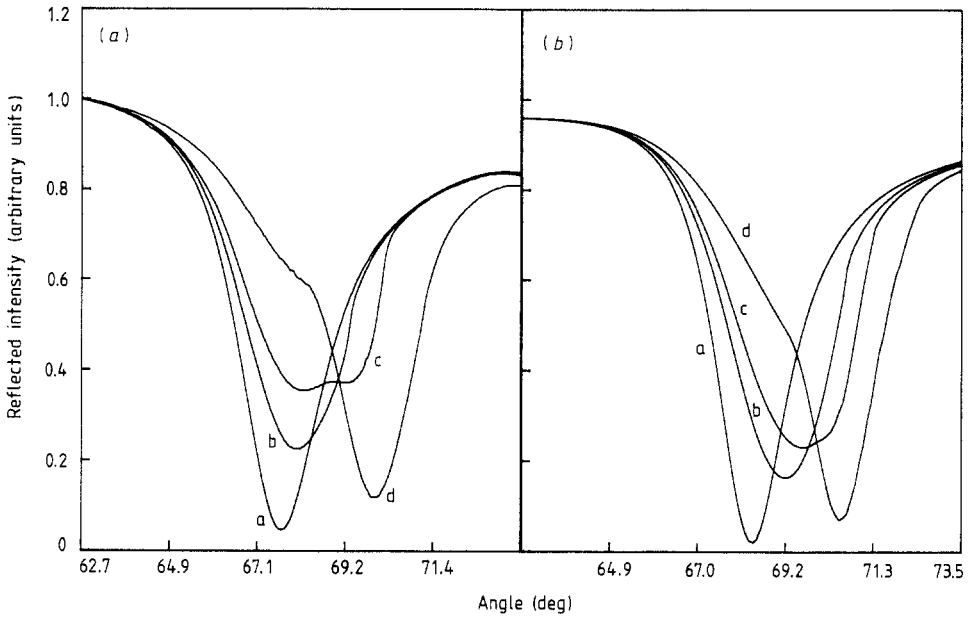

Figure 15. (*a*) Reflected intensity as a function of angle of incidence at an ambient temperature of 57.3°C for four incident powers: (curve a) 1 mW, (curve b) 3 mW, (curve c) 5 mW, (curve d) 8 mW. (*b*) Results of the theoretical modelling of the experimental situation of figure 15(*a*): (curve a) $I_{max} = 0.01$ (curve b) $I_{max} = 0.09$ (curve c) $I_{max} = 0.1325$ (curve d) $I_{max} = 0.24$. $\Delta I = 0.1$.

7.4. Raising of the ambient temperature

Figure 15(*a*) presents the observed reflectance responses for an unfocused beam of cross-sectional area 0.03 cm^2 for various incident powers, with the ambient temperature raised to 57.3°C. The response for an incident power of 1 mW (curve a of figure 15(*a*)) is that of the linear system with a deep reflectance minimum at $\sim 67.5°$. Increasing the power to 3 mW (curve b) produces a non-linear response similar to that of figure 11, although the minimum is now slightly deeper. Further increase to 5 mW results in the observation of two reflectance minima of approximately equal depth as shown in curve c, while curve d (for 8 mW incident power) shows a very strong minimum at an angle of $\sim 70°$ with a slight dip at an angle corresponding to the position of the minimum of curve a. The minimum of curve d corresponds to the liquid crystal in the isotropic phase. With this information it is possible to qualitatively understand the non-linear process.

For an incident power of 1 mW the heating of the liquid crystal is not sufficient for any visible non-linearity to occur. However, increasing the incident power to 3 mW is sufficient for part of the incident beam (the profile of which is that of a Gaussian distribution) to be intense enough to cause switching. The total observed response is an average of the responses of all the regions of the liquid crystal that are sampled by the beam, some of which are in the isotropic phase. On further increase of the incident power, the proportion of incident beam intense enough to cause non-linearity increases and, at an incident power of 8 mW, only a small proportion remains in the nematic phase, thus explaining the slight dip in curve d of figure 15(*a*). Curve c therefore approximately corresponds to half the liquid crystal in the beam being nematic and the remainder being isotropic.

7.5. Computer modelling including Gaussian spread

Dividing the temperature dependence of $\epsilon_\perp$ above 20°C and below 58°C into three regions of differing α, while assuming the value of ϵ in the isotropic phase to remain constant at $\epsilon = 2.492$ (see figure 14), it is now possible to closely model the experimental system by introducing a Gaussian spread in intensities. This is achieved by calculating the reflectance for perhaps 20 equally spaced intensities I (spacing ΔI), up to a maximum intensity, I_{max}. Using the normalised Gaussian distribution of the form

$$f(I) = (1/\sqrt{2\pi\sigma^2}) \exp[-(I - I_{max})^2/2\sigma^2] \tag{4}$$

the normalised average reflectance response, R, is given by

$$R = \left(\sum f(I) R(I) \Delta I\right) \left(\sum f(I) \Delta I\right)^{-1}. \tag{5}$$

The experimental system can then be modelled by varying I_{max} for an arbitrary σ (the standard deviation). Figure 15(*b*) shows the results of such a procedure for the data presented in figure 15(*a*) in the region where $\alpha = 0.131\ K^{-1}$. The similarity between the two figures is pleasing and confirms that a spread in incident intensities causes the raising and broadening of the reflectance minimum. The similarity is all the more pleasing when it is remembered that any thermal diffusion effects have been neglected.

Another contributory factor may be the variation of $\epsilon_\perp$ away from the interface. However, since the SPP fields only decay $\sim 1\ \mu m$ into the liquid crystal, such effects will be dominated by the temperature gradients in the plane of the interface. The two major differences between the corresponding curves of figure 15(*a*) and 15(*b*) are firstly that the two minima of curve c in figure 15(*a*) are not apparent in curve c of figure 15(*b*). Secondly, there is a pronounced 'kink' in curve d of figure 15(*a*) but the response is linear in figure 15(*b*), curve d. These two discrepancies are most probably due to the large discontinuity in ϵ that occurs at the clearing point so that there is not a linear increase in ϵ up to the isotropic value.

7.6. Self-diffraction

A further complication to this optical non-linearity is that the focusing of the incident laser beam onto the prism/silver interface causes the dielectric constant of the portion of liquid crystal at the centre of the spot to be significantly increased. Hence, diffraction rings will occur in the reflected beam as the incident beam diffracts off the self-induced dielectric constant profile. The shape and size of the diffraction pattern will depend

upon the angle of incidence, the incident intensity and the shape and position of the focal plane. Figures 16(*a*) and 16(*b*) show the observed diffraction pattern for a beam focused using a spherical lens at two different angles of incidence and figure 16(*c*) is that found using a cylindrical lens. Figures 16(*a*) and 16(*b*) illustrate the dependence on incident angle, while figure 16(*c*) shows a pattern analogous to a beam incident upon a narrow slit; for high (~20 mW) incident intensities thermal convection currents were also very noticeable. It should be noted that although these effects are a complication they are of little significance to the expected reflectance provided that all the reflected light is collected by the detector. (Figures 16 were taken by projecting the reflected beam onto a screen ~1 m from the sample.)

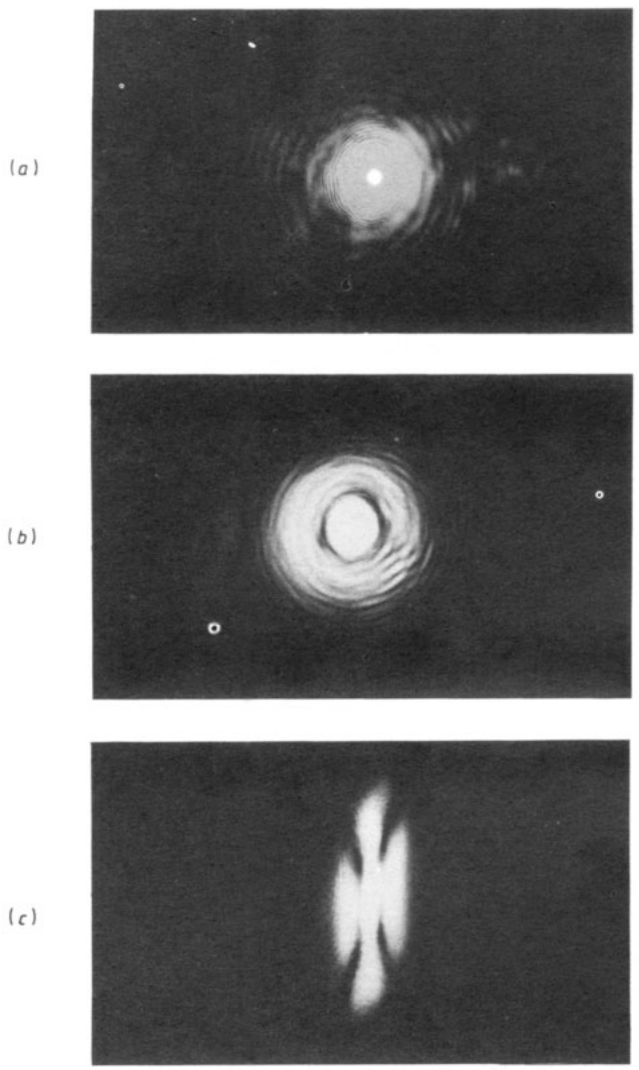

Figure 16. Self-diffraction patterns for: (*a*) spherical lens at an incident angle close to the switch of figure 11, (*b*) spherical lens at slightly greater angle, (*c*) cylindrical lens.

8. Initial conclusions

The mechanism of the optical non-linearity has been determined to be due to the warming of the nematic liquid crystal adjacent to the SiO_x through its clearing point, due to the energy loss of SPPs in the silver film. The raising and broadening of the reflectance minimum has been attributed to the Gaussian spread in incident intensities and incident angles, which thereby give a total response from liquid crystal at many temperatures. The spread in incident intensities and incident angles also causes self-diffraction to occur. Preliminary measurements of the response time of the non-linearity suggest that it is ~20 ms for an incident beam of 20.5 mW at a sample temperature of 20°C, although the question remains whether the response time will increase with decrease in incident power, since the time required to supply the required latent heat will increase.

Improvements to the sample design and fabrication and also to the experimental apparatus may now be suggested.

(i) In order to reduce the requirement for raising the ambient temperature to 57°C, a nematic liquid crystal should be used whose clearing point is closer to room temperature.

(ii) The volume of liquid crystal contained within the sample should be reduced so that convection currents (and thus cooling of the liquid crystal near to the interface) are minimised.

(iii) A small aperture (~0.5 mm) should be placed in the path of the incident beam so that a more uniform intensity distribution is obtained.

Having made these improvements more detailed measurements of the non-linearity are now possible.

9. Improved measurements

9.1. Choice of liquid crystal

Of all the liquid crystals available, it is the single-component liquid crystal, 4-6-alkyl-4′-cyanobiphenyl, commonly known as 6CB or K18, which has its clearing point closest to, and above, room temperature, with $T_c \simeq 29$°C. The general behaviour for both $\epsilon_\parallel$ and $\epsilon_\perp$ is the same (figure 17) as that of E7, in that there remains a large discontinuity in ϵ at $T_c = 28.3$°C, but the changes in dielectric constant at the phase transition are not as great—in other words, 6CB is less birefringent than E7. However, it was illustrated previously that a change of ~0.08 in ϵ is required to observe optical bistability, and so 6CB is sufficiently birefringent for non-linearities to be observed.

9.2. Sample fabrication

Reduction of the liquid crystal thickness was achieved by replacing the 50 μm thick mylar spacers of the previous sample with 2 μm thick aluminium foil spacers. The sample design is similar to that previously used, except that a pyramid prism geometry has now been used, thus allowing measurements to be made both with the liquid crystal director orthogonal to the plane of incidence and parallel to it, if required.

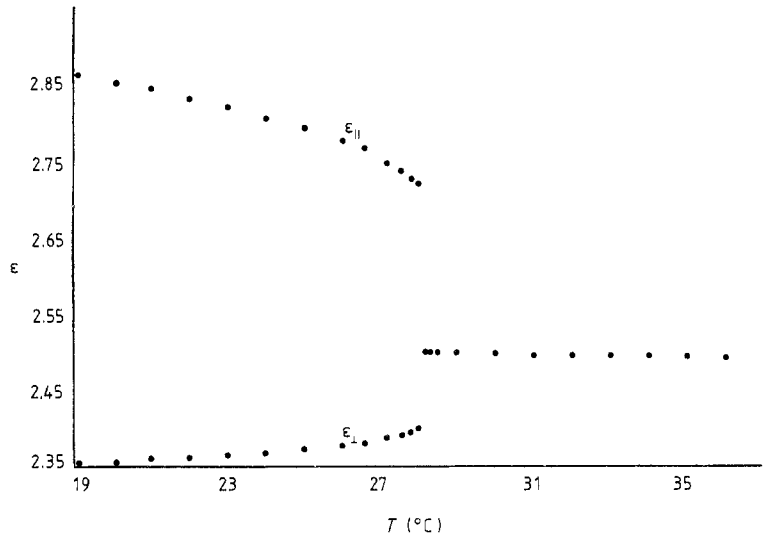

Figure 17. Optical dielectric constants of 6CB as a function of temperature at $\lambda = 589.6$ nm.

10. Results

10.1. Response with a focused beam at room temperature

With a 1 mm diameter aperture placed in the path of the beam, and using the 18.5 cm focal length lens to concentrate the incident radiation, the power was decreased in steps from 21 mW to 10 mW as shown in figure 18, at an ambient temperature of 20°C. For incident powers above 6 mW switching does occur and the increased sharpness of the switch, in comparison with data from the previous sample, is obvious. Undoubtedly, this is partly due to the decreased volume of the liquid crystal, but more significantly, the lowering of the phase transition temperature, so that a much higher fraction of liquid crystal is being warmed through the clearing point.

10.2. Response time of non-linearity

As before, the incident beam was modulated with a mechanical chopper and the reflectance response for different frequencies of modulation were recorded, but now for a range of incident powers. Figures 19(*a*) and 19(*b*) present the results for incident powers of 18 mW and 21 mW, respectively. From a study of the results of these measurements two points of interest can be made. Firstly, at a modulation frequency of 1600 Hz all the responses have reverted to the DC response for half the unmodulated incident power, and secondly, they all appear to revert to the 'half-power' response at the same frequency. Since the switching is due to warming of the liquid crystal through a first-order phase transition, the latent heat must be supplied. For low incident powers, the time required to supply the latent heat increases so that one would expect the response time to increase. However, the amount of liquid crystal being warmed through the clearing point will be less, so that the response time will remain much the same as for higher powers, provided that the Gaussian distribution in incident intensities remains constant. The modulated incident beam reflectance response will revert to that of the half-power DC response when the response time of the non-linearity

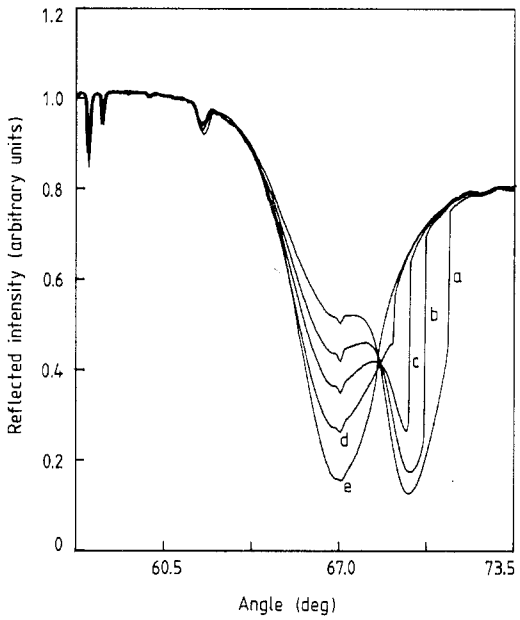

Figure 18. Reflectivity from the sample for a variety of incident powers of the focused beam: (curve a) 21 mW, (curve b) 18 mW, (curve c) 15 mW, (curve d) 9 mW.

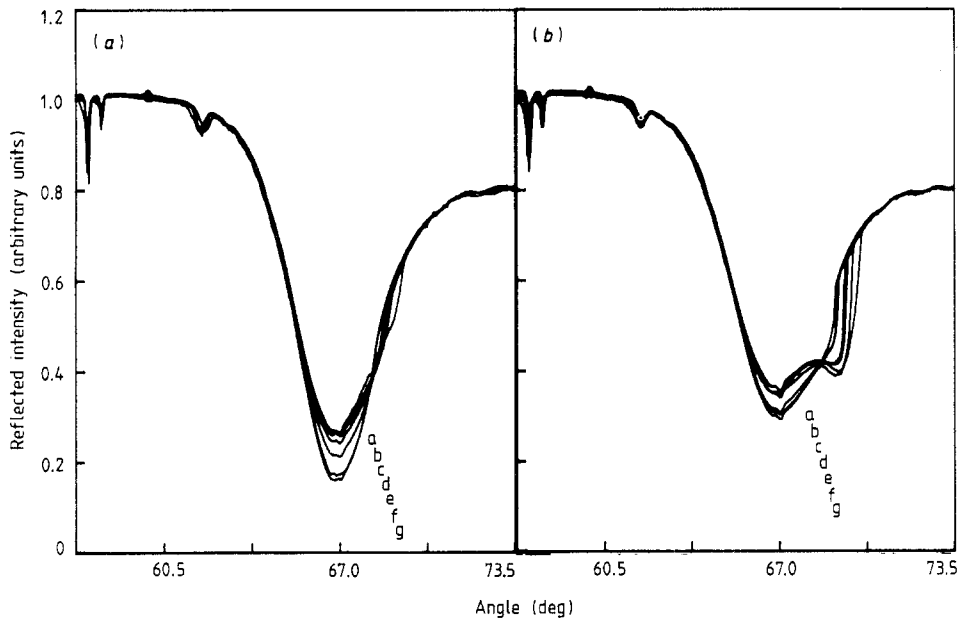

Figure 19. (*a*) Reflected intensity as a function of angle of incidence for a focused incident beam of 18 mW power at different frequencies of modulation: (curve a) 100 Hz, (curve b) 400 Hz, (curve c) 800 Hz, (curve d) 1200 Hz, (curve e) 1600 Hz. (*b*) Reflected intensity as a function of angle of incidence for a focused incident beam of 21 mW power at different frequencies of modulation: (curve a) 100 Hz, (curve b) 400 Hz, (curve c) 800 Hz, (curve d) 1200 Hz, (curve e) 1600 Hz.

is greater than that of the time of modulation. A simple analysis shows (Innes 1987) that the growth and decay times of the non-linearity are approximately equal and ~20 ms.

10.3. Raising of the ambient temperature

Once again the sample was warmed above room temperature to eliminate the use of the converging lens. Figure 20 presents five sets of data for an unfocused incident beam of 22 mW power at increasing ambient temperatures. As the bulk of the liquid crystal is warmed and its dielectric constant increases, so the guided modes present at angles of incidence below the SPP resonance angle move position to higher angles of incidence. The expected switching occurs in data recorded at $T = 26.9°C$ and 28°C, most of the liquid crystal being warmed into the isotropic phase in the latter case. At $T = 29.1°C$, all of the liquid crystal is in the isotropic phase. However, it is evident that the Gaussian spread in incident intensities is still causing the lifting of the reflectance minimum. One would like to observe a sharp switch down to the fully isotropic reflectance response, as predicted by theory.

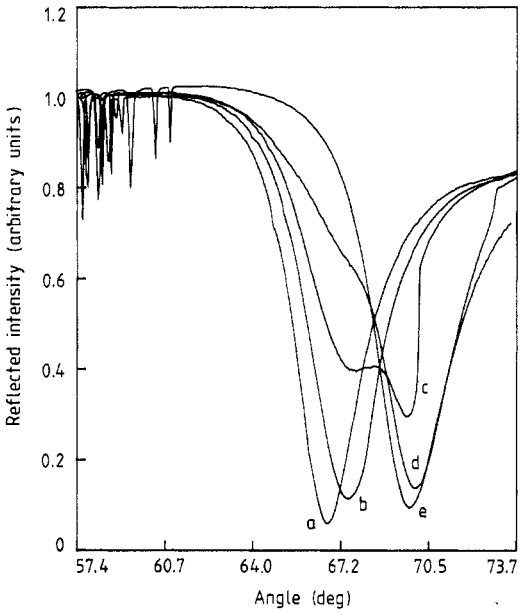

Figure 20. Reflected intensity as a function of angle of incidence for an unfocused beam power of 22 mW at increasing ambient temperatures: (curve a) 21.4°C, (curve b) 26.0°C, (curve c) 26.9°C, (curve d) 28.0°C, (curve e) 29.1°C.

10.4. 'AC-on-DC' probe experiment

In an attempt to record the reflectance response from just the central portion of the incident beam, the experimental arrangement shown in figure 21 was constructed, involving the use of both a DC beam from the 50 mW He–Ne laser (the 'pump' beam) and a beam from a 10 mW He–Ne laser (the 'probe' beam) which was modulated using a mechanical chopper. A converging lens of focal length 40 cm was used to focus the probe beam to a spot size of diameter 400 μm, positioned at the centre of the pump

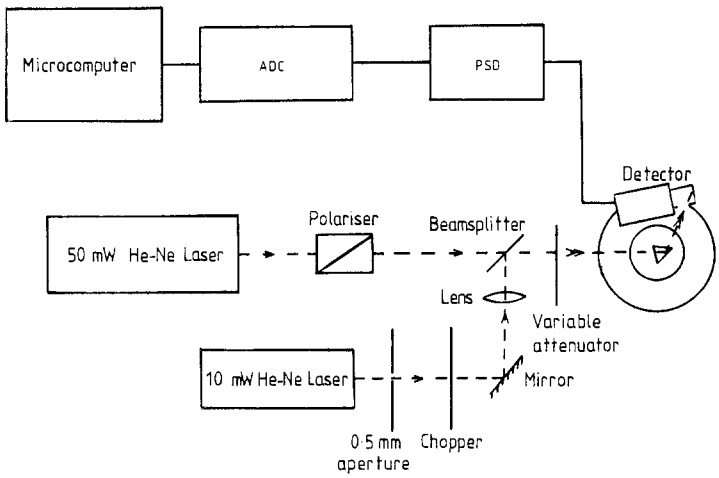

Figure 21. Experimental apparatus for the 'AC-on-DC' probe experiment.

beam spot (of diameter 2 mm) at the prism/silver interface. The probe beam was attenuated so that its DC power level was ~300 times less than that of the pump beam. The signal from the silicon photodiode detector consisted therefore of a large DC signal with a small AC signal superimposed. Using a PSD, the AC signal could be separated from the DC signal and the reflectance response of the probe beam recorded. Since the probe beam would not cause any non-linearity itself, it was hoped that it would sample any non-linearity caused by the pump beam, at the centre of that beam—edge effects should be negated. Figure 22 presents reflectance data for a variety of pump beam powers at a temperature of 26.5°C. It can be seen that the raising of the reflectance minimum and the appearance of two minima still occurs. However, comparison of this type of data with previously taken data does show that the degree of raising has been reduced. That two minima may still be observed, however, means that the probe beam is sampling a range of temperatures of liquid crystal, although the range has been reduced. As previously explained, it is extremely unlikely that a distribution in liquid crystal temperatures normal to the interface can be responsible for the observed reflectance responses. The explanation lies in the fact that although all the liquid crystal region sampled by the probe beam has been warmed into the isotropic phase, some will cool into the nematic phase, influenced by the cooler surrounding regions, as the angle of incidence is swept to lower angles, i.e. the response is not that of a closed system. The greater the incident power, then the further the liquid crystal will be warmed into the isotropic phase, so that as the incident angle is decreased below the isotropic phase SPP resonance angle, the greater the range of temperatures of liquid crystal present as some begins to cool. This fact is illustrated in figure 22; the small dip or kink associated with the nematic phase becomes broader as the incident power of the pump beam is increased. It can therefore be concluded that, in order to observe the response from a totally isothermal region, it is necessary for the pump beam cross-sectional area to be much greater than that of the probe beam than is the case in this experiment. Since increasing the area of the pump beam will greatly reduce the incident intensity, the liquid crystal sample would have to be kept at a temperature extremely close to the phase transition temperature, a situation that is beyond the specifications of the

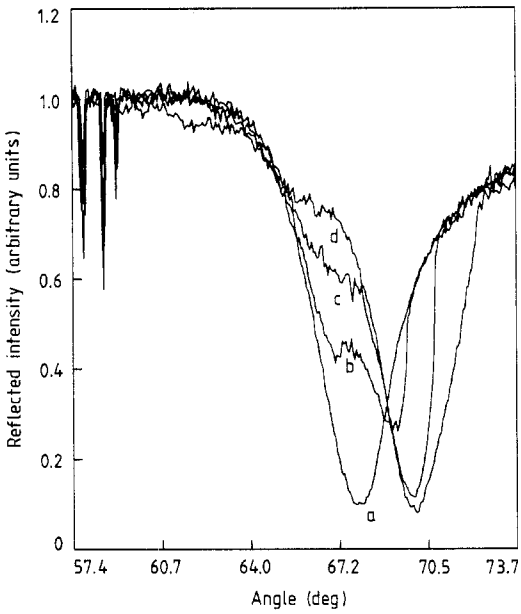

Figure 22. Reflected intensity of the probe beam as a function of incident angle for differing values of pump beam power at a temperature of 26.5°C: (curve a) 6 mW, (curve b) 7 mW, (curve c) 10 mW, (curve d) 14 mW.

experimental apparatus available.

10.5. Behaviour of Fabry–Perot modes and critical opalescence

A study of the behaviour of the Fabry–Perot (FP) modes in the liquid crystal layer may yield further information on the behaviour of the liquid crystal. Figures 23 present the reflectance responses for a pump beam power of 0.1 mW for temperatures within 0.5°C of the clearing point; a change in phase is not expected unless very close to the transition temperature. A careful examination of these data shows that as the temperature is increased so the SPP reflectance minimum moves to higher angles of incidence, corresponding to an increase in dielectric constant, and similarly for the bulk FP modes. However, it should be noted that the FP mode reflectance dips broaden significantly without there being any broadening of the SPP response. Further increase in temperature shows a broadening in the SPP resonance dip and then a return to the expected isotropic response, with sharp dips corresponding to FP modes in the isotropic phase. One must therefore ask what is the cause of the broadening of bulk and surface modes.

The broadening of the SPP response could be attributed to a range of liquid crystal temperatures. However, the response does not show any skewness or double-dip behaviour but simply a raising and broadening. This therefore suggests that the behaviour is simply due to an increase in scattering within the liquid crystal due to critical opalescence (McMillan 1975)—the formation of droplets of nematic phase in the isotropic phase—which is a common phenomenon near to phase transitions. (That the broadening occurs firstly in the bulk FP modes is probably due to a temperature drift with time and not to any difference in phase transition temperature between bulk and surface regions.)

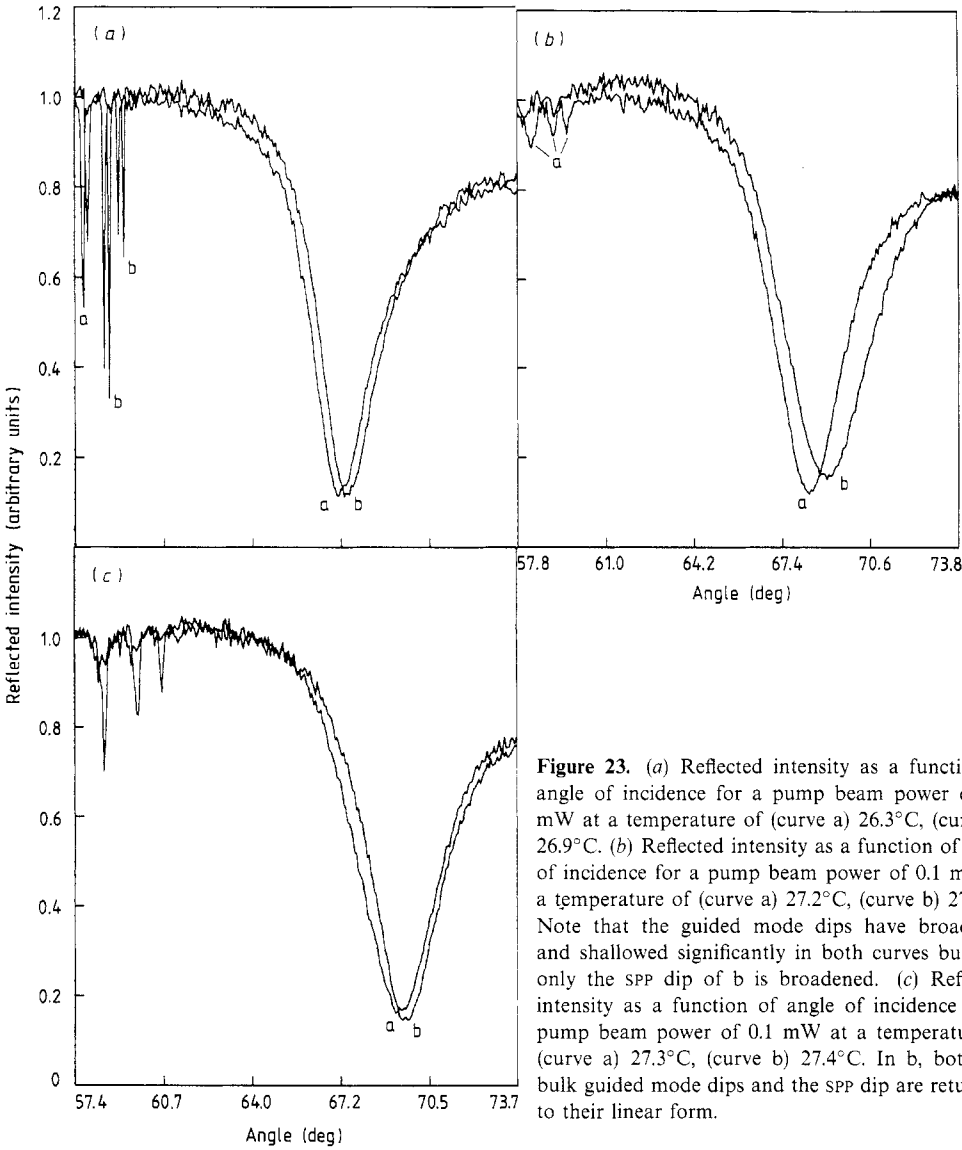

Figure 23. (*a*) Reflected intensity as a function of angle of incidence for a pump beam power of 0.1 mW at a temperature of (curve a) 26.3°C, (curve b) 26.9°C. (*b*) Reflected intensity as a function of angle of incidence for a pump beam power of 0.1 mW at a temperature of (curve a) 27.2°C, (curve b) 27.3°C. Note that the guided mode dips have broadened and shallowed significantly in both curves but that only the SPP dip of b is broadened. (*c*) Reflected intensity as a function of angle of incidence for a pump beam power of 0.1 mW at a temperature of (curve a) 27.3°C, (curve b) 27.4°C. In b, both the bulk guided mode dips and the SPP dip are returning to their linear form.

10.6. Orthogonal director orientation

With the liquid crystal director aligned parallel but now in the plane of incidence, the electromagnetic fields sample both $\epsilon_{\parallel}$ and $\epsilon_{\perp}$, so that the system is uniaxially birefringent and can be modelled using Sprokel's approach (Sprokel 1981). Using this theory it is possible to predict the position of the SPP reflectance minimum in the nematic phase at 27.15°C and it is found that the minimum lies at a higher angle than for the previous director orientation, so that the change in effective dielectric constant at the phase transition is now not as great, perhaps corresponding to an increase in effective dielectric constant of 0.04. Therefore, one would not expect any switching to occur at this ambient temperature.

Figure 24 presents data taken for this orientation for a variety of powers of pump beam, and indeed no switching occurs; switching would occur at lower ambient

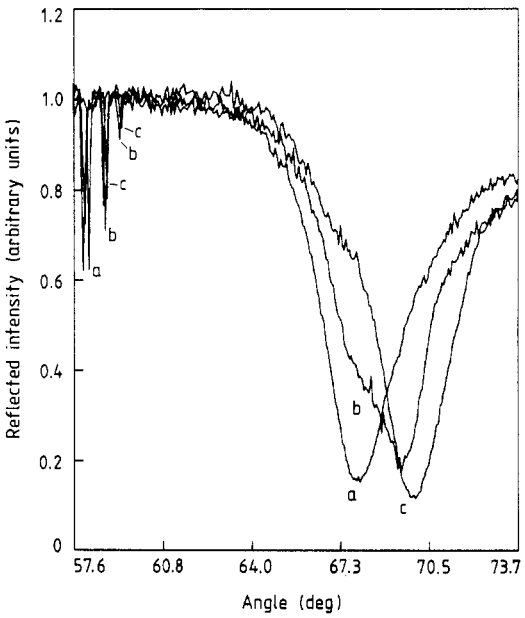

Figure 24. Reflectivity as a function of incident angle at an ambient temperature of 27.15°C with incident pump beam powers of: (curve a) 0.1 mW, (curve b) 4 mW, (curve c) 6 mW.

temperatures. However, one is then led to ask what would be the response if the liquid crystal were homeotropically aligned. In this situation the electromagnetic fields of the SPP mode would sample mainly $\epsilon_{\|}$, resulting in a SPP reflectance minimum at a much higher angle of incidence and a much larger change in dielectric constant at the phase transition. The liquid crystal will now have a negative non-linear coefficient since the nematic SPP dip lies above the isotropic dip. Metal surfaces may yield homeotropic alignment (Cognard 1981) and this was found to be so for the bare silver of this sample. Reflected intensity data for the homeotropically aligned liquid crystal is presented in figures 25 (Innes *et al* 1988), where figure 25(*a*) presents reflected intensity data taken as function of incident angle and shows the two well-separated SPP resonance dips. It is apparent that the change in reflectivity that will occur at switching will be much greater than previously seen, and this fact is illustrated in reflectance versus intensity data presented in figure 25(*b*).

11. Summary and conclusions

It has been shown that an aligned nematic liquid crystal layer, combined with a thin silver film in the Kretschmann–Raether configuration, allows the observation of a large thermally induced optical non-linearity. The non-linearity is due to the warming of liquid crystal close to the silver film through the clearing point by energy loss of SPPs at the silver surface. Optical bistability with angle of incidence and incident intensity are both observed.

After a detailed account of optical bistability in reflection using SPPs, it has been shown that while past theoretical works have concentrated upon the reorientational effect (Kerr effect) in materials (Wysin *et al* 1981, Martinot *et al* 1984, Agarwal and Gupta 1986a, b) experimental reports of optical bistability using SPPs have been due

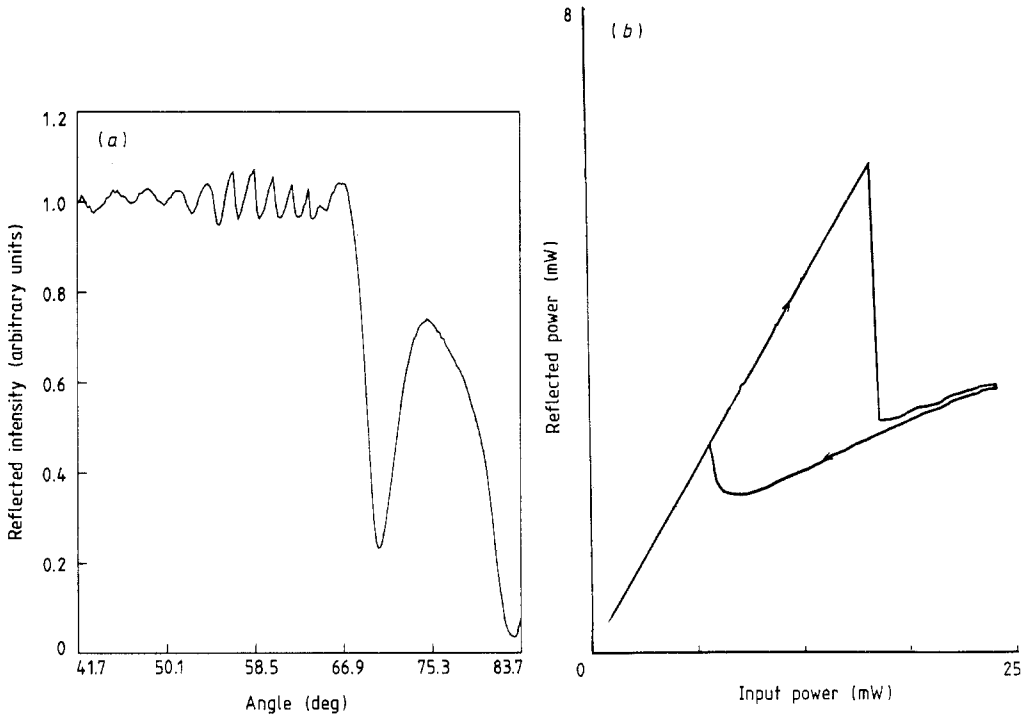

Figure 25. (*a*) Reflected intensity as a function of incident angle for the homeotropically aligned 6CB liquid crystal cell. Note that although in previously presented data loss of incident power at the entrance face of the prism due to reflection was only ~3% , now it is ~50% . (*b*) Reflected power as a function on incident power for the homeotropically aligned liquid crystal cell, illustrating the greater depth of the switch now obtained (Innes *et al* 1988). Angle of incidence is 69.9°.

to a thermally induced non-linearity (Martinot *et al* 1985, Innes and Sambles 1987). In the former work, the rise in local temperature was estimated to be ≃13 K (for an intensity ≃ 3×10^{-3} W cm^{-2}) with switch-up and switch-down times of ≃ 100 ms and ≃ 150 ms respectively. In the work presented here, results similar to those of Martinot *et al* (1985) have been obtained but, in this case, it has been shown that the temperature rise for an incident intensity of ~ 40 W cm^{-2} is approximately 40 K, with an initial estimate of the response time of ~20 ms. The ambient temperature was raised to just below the clearing point so that an unfocused incident beam could be used, enabling the observation of a large non-linearity for intensities ≃ 0.2 W cm^{-2}. The broadening and raising of the recorded reflectance versus incident angle responses are attributed to a spread in temperatures of the liquid crystal due to the transverse Gaussian distribution intensity profile of the incident beam and also to temperature gradients in the liquid crystal caused by convection currents. A computer program was developed to include a Gaussian spread of liquid crystal temperatures, which resulted in good qualitative modelling of the non-linear response.

An improved sample design, with a thinner liquid crystal layer and using a nematic liquid crystal (6CB) whose clearing point was closer to room temperature than that of E7, enabled a more comprehensive study of the non-linearity. Very sharp switches were observed in reflectance versus incident-angle data, resulting from the lowering of the clearing point. Further, a more detailed study of the response time of the non-linearity

confirmed the original estimate of ~20 ms. Attempts to obtain the reflectance response of a closed region of liquid crystal using a novel 'AC-on-DC' probe technique succeeded in reducing the sampled Gaussian spread in temperatures of liquid crystal but it was concluded that a much broader 'pump' beam would be necessary to eliminate the spread, but this was not possible to achieve with equipment available. The reflectance responses for homogeneous alignment in the plane of incidence and also homeotropic alignment have been presented. For the former the maximum change in average dielectric constant was not sufficient for bistability to occur at the particular ambient temperature, but for the latter (Innes *et al* 1988) a much larger change in dielectric constant was possible, allowing a large bi-stable loop to be observed. However, the nematic phase SPP resonance dip for this alignment lies at very high angles of incidence ($\simeq 80°$) and so about 50% of light incident upon the prism is reflected at the entrance face. This problem could be overcome by designing a new shape of prism or, more practically, by using one of the new lower refractive index nematic liquid crystals that have recently been developed.

Conclusions that can be drawn from the work presented in this paper are as follows.

(i) Although theoretical treatments of the observation of optical bistability using SPPs have concentrated upon the optical Kerr effect, experimental results (Innes and Sambles 1987, Martinot *et al* 1985) indicate that thermally induced non-linearities will nearly always dominate.

(ii) If one wishes to observe reorientational effects, in a nematic liquid crystal perhaps, then the Fabry–Perot interferometer geometry or guided mode geometry are preferable, provided that no highly absorbing media (i.e. metals) are present. The SPP geometry is ideal for thermally induced non-linearities.

(iii) The thermal conductivities of the surrounding media have to be chosen carefully in order to optimise the desired properties.

(iv) The only situation in which thermal effects are unlikely to be significant, at high incident intensities, will be the Otto geometry, where the bulk metal will conduct the heat away from the interface. Therefore, it may be wise to perform experiments such as the observation of second-harmonic generation in organic layers using SPPs (Girling *et al* 1986) in the Otto configuration.

(v) The incident intensities required to observe bistability would be drastically reduced if the LRSPP mode (Sarid 1981) were excited. The narrow resonance dip associated with this mode means that a much smaller change in dielectric constant is required to observe optical bistability and so the need to warm the liquid crystal through the clearing point would be removed. The experimental geometry required to excite the LRSPP mode is, however, complicated and there are many practical problems (Innes 1987).

(vi) The response times observed in the current experiment ($\simeq$ 20 ms) inhibit the device potential for this structure, except perhaps as a laser-power limiter.

(vii) It should also be noted that the 'AC-on-DC' probe technique has illustrated the ease with which one beam may be switched by another using the simple Kretschmann–Raether configuration.

Acknowledgments

The authors are grateful to the SERC for the support of both a CASE award for RAI and a research grant to enable the purchase of equipment required for the experiments.

References

Abraham E and Smith S D 1982 *Rep. Prog. Phys.* **45** 815
Agarwal G S and Gupta S D 1986a *Optical Bistability III* (Berlin: Springer) p 117
——1986b *Phys. Rev.* B **34** 5239
Arakelyan S M, Chilingaryan Yu, Grigorian G L, Lyakhov G A, Nersisyan S Ts and Svirko Yu P 1981 *Mol. Cryst. Liq. Cryst.* **71** 137
Arakelyan S M, Grigorian G L, Kocharian L M, Nersisyan S Ts and Chilingaryan Yu 1986 *Phys. Lett.* **118A** 254
Barnes W L and Sambles J R 1986 *Surf. Sci.* **177** 399
Boardman A D 1982 *Electromagnetic Surface Modes* ed. A D Boardman (Chichester: Wiley) p 17
Cognard J 1981 *Mol. Cryst. Liq. Cryst.* **78** Supplement
Durbin S D, Arakelian S M, Cheung M M and Shen Y R 1982 *Opt. Lett.* **7** 145
Durbin S D 1984 *PhD Thesis* University of California, Berkeley
Girling I R, Cade N A, Kolinsky P V, Cross G H and Peterson I R 1986 *J. Phys. D: Appl. Phys.* **19** 2065
Innes R A 1987 *PhD Thesis* University of Exeter
Innes R A, Ashworth S P and Sambles J R 1988 *Phys. Lett.* **A** Submitted
Innes R A and Sambles J R 1985 *Solid State Commun.* **56** 493
—— 1987 *Opt. Commun.* **64** 288
Innes R A, Welford K R and Sambles J R 1987 *Liq. Cryst.* **2** 843
Kaplan A E 1977 *Sov. Phys.—JETP* **45** 896
Khoo I C 1982 *Appl. Phys. Lett.* **41** 909
Khoo I C and Shen Y R 1985 *Opt. Eng.* **24** 579
Khoo I C and Zhuang S L 1980 *Appl. Phys. Lett.* **37** 3
—— 1982 *IEEE J. Quant. Electron.* **QE-18** 246
Kretschmann E and Raether H 1968 *Z. Naturf.* a**23** 2135
Lloyd A D, Janossy I, MacKenzie H A and Wherrett B S 1987 *Opt. Commun.* **61** 339
Martinot P, Koster A and Laval S 1985 *IEEE J. Quant. Electron.* **QE-21** 1140
Martinot P, Laval S and Koster A 1984 *J. Physique* **45** 597
McMillan W L 1975 *J. Physique Coll.* **1** 103
Otto A 1968 *Z. Phys.* **216** 398
Sambles J R and Innes R A 1988 *J. Mod. Opt.* **35** 791
Sarid D 1981 *Phys. Rev.* B **47** 1927
Shelton J W and Shen Y R 1970 *Phys. Rev. Lett.* **25** 23
Smith P W, Herman J P, Tomlinson W J and Maloney P J 1979 *Appl. Phys. Lett.* **35** 846
Sprokel G J 1981 *Mol. Cryst. Liq. Cryst.* **68** 39
Welford K R, Sambles J R and Clark 1987 *Liq. Cryst.* **2** 91
Wysin G M, Simon H J and Deck R T 1981 *Opt. Lett.* **6** 30
Zel'dovich B Ya, Pilipetskii N F, Sukhov A V and Tabiryan N V 1980 *JETP Lett.* **31** 263